Structure induced tunable magnetic properties of Zn substituted $Mn_{1-x}Zn_xFe_2O_4$ ($x = 0$–1) NPs

Navjot Kaur[1], *Bhupendra Chudasama*[2] ✉

[1]*Laboratory of Nanomedicine, Thapar University, Patiala 14700, India*
[2]*School of Physics and Materials Science, Thapar University, Patiala 14700, India*
✉ *E-mail: bnchudasama@gmail.com*

Published in Micro & Nano Letters; Received on 1st September 2016; Accepted on 14th November 2016

$Mn_{1-x}Zn_xFe_2O_4$ nanoparticles (MZ NPs) owing to their Zn content dependent tunable magnetic properties have potential applications in energy conversion devices and in nanomedicine. It is a well-recognised fact that magnetism of MZ NPs has critical dependence on degree of Zn substitution at tetrahedral sites. In addition, the role of cation distribution between the tetrahedral and octahedral sites for a particular degree of Zn-substitution, i.e. the degree of inversion (δ) also influences their magnetic characteristics. However, the exact correlation between distribution of bivalent metal ions between tetrahedral and octahedral sites and corresponding magnetic characteristics is not well understood. In order to explore this structural dependence of magnetic characteristics of MZ NPs, a series of $Mn_{1-x}Zn_xFe_2O_4$ ($x = 0-1$) nanoparticles have been synthesized by chemical co-precipitation method. Saturation magnetisation and Curie temperature of MZ NPs are strongly correlated with the degree of inversion and exchange interactions between the magnetic ions, while the coercivity and remanence is independent of it and only depends on crystallite size. Both saturation magnetisation and Curie temperature decreases with increasing Zn substitution into spinel matrix. This could be attributed to the weakening of strong (A-B) inter lattice super exchange interaction instead partial substitution of Zn at octahedral Mn sites.

1. Introduction: In recent years, $Mn_{1-x}Zn_xFe_2O_4$ ($x = 0$–1) nanoparticles (MZ NPs) have attracted considerable interest because of their technological importance in magnetic hyperthermia, magnetic resonance imaging, data storage, spintronics, sensors [1, 2] etc. They are also used in power transformers: choke coils, noise filters and recording heads [3]. It is also being considered as one of the promising candidate for the preparation of magnetic fluids for heat transfer and energy conversion devices [4, 5]. MZ NPs possess interesting magnetic properties such as high magnetic permeability and low core losses in addition to strong zinc (Zn)-content dependent saturation magnetisation and Curie temperature. Magnetism in MZ NPs largely depends on the degree of Zn substitution in spinel lattice, synthesis method used and the conditions of preparation. MZ NPs are being synthesised by various bottom-up techniques such as hydrothermal [6], sol–gel [7], microemulsion [8], co-precipitation [9] etc. each showing different magnetic characteristics, the origin of which always remained unsettled [6–9].

MZ NPs are ferrimagnetic. They possess cubic spinel structure with general formula AB_2O_4, where A and B refer to the tetrahedral and octahedral cation sites, respectively. Type of cations and their distribution between the two interstitial sites in the spinel unit cell determine their intrinsic magnetic properties [10, 11]. This cation distribution depends on the ionic radii of the cation [12]. $ZnFe_2O_4$ (i.e. $x = 0$) has normal spinel structure, where Zn^{2+} occupies the tetrahedral sites due to its affinity for sp^3 bonding with oxygen anions, leaving all the ferric ions at the octahedral sites. Owing to this the only possible interaction between the ferric ions is intra-lattice (B–B) exchange interaction. Since (B–B) exchange interaction is very weak, $ZnFe_2O_4$ NPs are paramagnetic at room temperature [13]. On the other hand, $MnFe_2O_4$ has mixed spinel structure with degree of inversion, $\delta \simeq 0.2$. In this case manganese (Mn) and ferric ions occupy both the tetrahedral A-sites and octahedral B-sites. It was previously reported that MZ NPs possess mixed spinel structure as cations Me^{2+} and Fe^{3+} occupy both the interstitial sites [14–16]. Attia [17] has reported the cation distribution in MZ NPs. In MZ NPs, Zn ions always occupy the A-sites while Fe and Mn ions are distributed between A- and B-sites. This distribution of Mn and Fe ions depends on the degree of inversion and the Zn-content at A-site. Xuan *et al.* [18] have reported increase in saturation magnetisation of MZ NPs for small Zn substitution at A-sites followed by a decrease in their saturation magnetisation for higher Zn substitution. However, they could not reveal the strong magnetisation dependence of MZ NPs on Zn-content at interstitial sites and role of cation distirbutions. Rath *et al.* have also reported that the particle size, lattice parameter and magnetic properties of MZ NPs dependents on cation distribution. They have denoted decrease in particle size and lattice parameter with increase in Zn concentration in terms of the transformation from mixed spinel to normal spinel structure; however, they failed to provide any experimental evidence for it. In addition, they could not explain the observed magnetisation dependence of MZ NPs on degree of zinc (Zn) substitution in the spinel matrix [19]. Gopalan *et al.* have reported the impact of Zn substitution on the structural and magnetic properties of chemically derived nanosized MZ ($x = 0$–1). They have observed increase in magnetisation of MZ NPs for $x = 0.2$–0.4 followed by a decrease; however, they could not correlate it with the corresponding structural changes taking place in the spinel matrix of MZ NPs due to variation in the Zn substation at interstitial sites [20]. Varshney *et al.* [21] have studied the effect of site occupancy and cation ordering on structural and vibrational properties of $Zn_xMn_{1-x}Fe_2O_4$, but no study on their magnetic properties have been conducted.

From the literature survey it has been found that the role of cations vis-a-vis their occupancies at tetrahedral and octahedral sites are not clear as regards to their influence in deciding the overall magnetic properties of MZ NPs is concern. It is in this context a study of structural dependence of magnetic properties of MZ NPs with varying degree of Zn substitution assume significance. This Letter probes the influence of Zn substitution on magnetic properties (magnetisation, coercivity, remanence and Curie temperature) of chemically co-precipitated MZ NPs and their correlation with structural changes in the unit cell caused by varying cation distribution between tetrahedral and octahedral interstitial sites.

2. Materials and methods

2.1. Materials: AR grade $FeCl_3$ was obtained from S.D. fine-chem Ltd., $MnCl_2.4H_2O$ was purchased from LOBA chemicals. $ZnSO_4.7H_2O$, NaOH and acetone were purchased from Merck, India. All chemicals were used as-received without any purification. Aqueous solutions were prepared in Milli-Q ultrapure water ($\rho = 18.2$ MΩ).

2.2. Synthesis of MZ ($x = 0$–1) NPs: A series of MZ ($x = 0$–1) (MZ NPs) NPs were synthesised by chemical co-precipitation of Fe^{3+}, Mn^{2+} and Zn^{2+} from their aqueous salt solutions [22, 23]. Aqueous solutions of $MnCl_2.4H_2O$, $ZnSO_4.7H_2O$ and $FeCl_3$ were prepared by dissolving stoichiometric quantities of these salts in 300 ml distiled water. pH of the solution was adjusted to <2 with dilute HCl. It was then added under constant stirring into 100 ml aqueous solution of NaOH. The molar ratio of ($MnCl_2.4H_2O$ + $ZnSO_4.7H_2O$):$FeCl_3$:NaOH was maintained as 1:2:8. The solution pH was then adjusted to 11 with 1 M NaOH. It was stirred for 20 min. During this, metal salts get converted into their hydroxides

$$(1-x)\ Mn^{2+} + x\ Zn^{2+} + 2Fe^{3+} + 8OH^- \xrightarrow{93^\circ C} (1-x)Mn(OH)_2\ x\ Zn(OH)_2\ 2Fe(OH)_3 \quad (1)$$

These metal hydroxides were then subjected to constant heating at 90°C for 3 h. During this time hydroxides transform to NPs of metal oxides [24]

$$(1-x)\ Mn(OH)_2 x\ Zn(OH)_2\ 2Fe(OH)_3 \xrightarrow{90^\circ C/3\,h} Mn_{(1-x)}Zn_xFe_2O_4 + nH_2O \quad (2)$$

Magnetic NPs were cooled to room temperature, magnetically decanted and washed multiple times with warm distiled water. The resulting black precipitates were washed with acetone and dried overnight at 80°C.

3. Characterisation of MZ NPs: X-ray diffraction (XRD) studies of MZ NPs were carried out on PAN analytical X'pert PRO powder X-ray diffractometer. The X-ray diffractograms were recorded at room temperature by using monochromatic CuKα radiation (λ = 1.5405 Å) in the 2θ range of 28°–70°. Diffractograms were further refined by Rietveld refinement method by using Fullprof suite programme. In the refinement, diffraction patterns were modelled by pseudo-Voigt function. The assumed structure model is spinel with space group Fd3m. Bivalent (Mn^{2+}; Zn^{2+}) and trivalent (Fe^{3+}) metal ions occupy the Wyckoff 8a and 16d special positions, respectively and oxygen atoms are in 32e special positions. To find out degree of inversion (δ) of bivalent metal ions (Mn^{2+}) between tetrahedral and octahedral sites, the site occupancies of Mn^{2+}, Zn^{2+} and Fe^{3+} ions were refined with an assumption that the ratio of site occupancies of A- and B-sites are A:B = 1:2. The quality of fit is confirmed by the goodness of fit, χ^2 and reliability factors, R_p and R_{wp} which represents the weighted differences between measured and calculated diffraction patterns. Transmission electron microscopy (TEM) image and specific area electron diffraction (SAED) pattern of MZ NPs was recorded on JEOL GEM 200 transmission electron microscope, which was operated at 200 kV. Sample for TEM was prepared by putting a drop of NP suspension in ethanol on carbon coated copper grid. It was then vacuum dried overnight. Magnetisation measurements of MZ NPs were carried out in the magnetic field range of −4.5 KOe to 4.5 KOe on Lake Shore 7404 vibrating sample magnetometer (VSM) at 25°C. The Curie temperatures of MZ NPs were also determined from temperature dependent magnetisation measurements. Magnetisation as a function of temperature (M–T) was measured on 7404 VSM by using Lakeshore 74,035 single-stage cryostat oven assembly. The measurements were performed from 300 to 600 K.

4. Results and discussion: Magnetic characteristics of MZ NPs depend on the degree of Zn substitution and distribution of bivalent metal ions between tetrahedral and octahedral sites. To probe this structural dependence, powder X-ray diffractograms of MZ NPs were recorded. Fig. 1 shows the refined X-ray diffractograms of as-synthesised MZ NPs. In each diffractogram six peaks were observed, which are indexed well with the spinel structure (space group Fd3m) [20, 25].

Obtained best fit values of various structure factors and goodness of fit parameters (χ^2, R_p R_{wp}) are reported in Table 1.

In normal spinel lattice, all the bivalent metal ions occupy the tetrahedral sites while all the octahedral sites are occupied by the trivalent metal ions. In inverse, spinel half of the bivalent metal ions occupy the tetrahedral sites while rest of them occupies the octahedral sites and trivalent metal ions occupy the octahedral sites. In mixed metal ferrite, both bivalent and trivalent metal ions occupy both the tetrahedral and octahedral sites with different degrees of occupancies. In MZ ferrite, which is mixed metal ferrites, bivalent metal ions partially occupy both the tetrahedral and octahedral sites. It is observed from refined data that the lattice parameter of MZ NPs increases with increasing Zn-content. This might be because of the difference in the ionic radii of bivalent and trivalent metal ions occupying the tetrahedral and octahedral sites in spinel lattice leading to different degrees of lattice strain into the

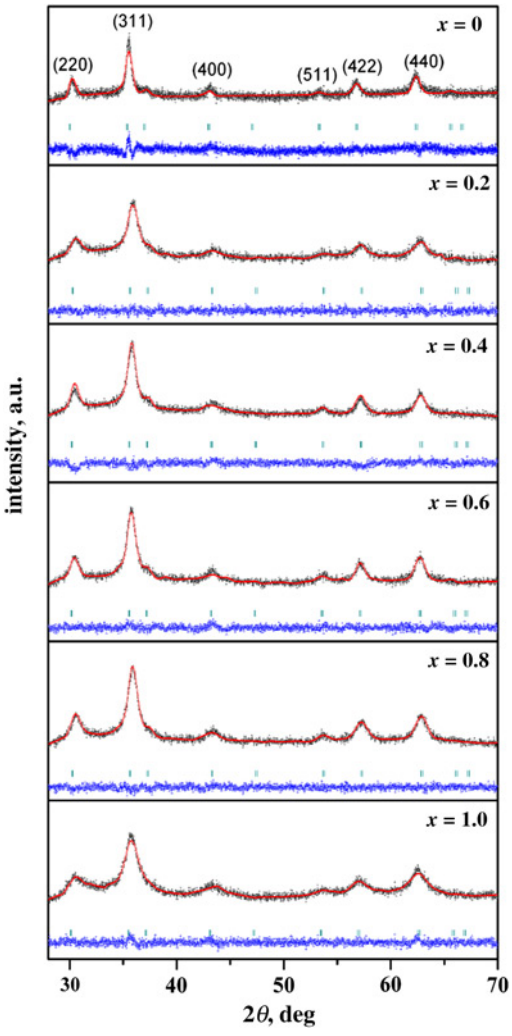

Fig. 1 *Rietveld refined XRD patterns of $Mn_{1-x}Zn_xFe_2O_4$ (x = 0–1) NPs*

doi: 10.1049/mnl.2016.0555

Table 1 Degree of inversion of MZ NPs

Sample	Degree of inversion, δ	Lattice parameter	R_p	R_{wp}	χ^2
$Mn_{1.0}Zn_{0.0}Fe_2O_4$	0.22	8.41838	17.5	18.5	1.3
$Mn_{0.8}Zn_{0.2}Fe_2O_4$	0.32	8.35689	1.12	1.40	1.1
$Mn_{0.6}Zn_{0.4}Fe_2O_4$	0.28	8.36746	12.7	17.1	1.3
$Mn_{0.4}Zn_{0.6}Fe_2O_4$	0.15	8.37792	2.92	4.04	1.1
$Mn_{0.2}Zn_{0.8}Fe_2O_4$	0.19	8.357486	3.62	4.15	1.1
$Mn_{0.0}Zn_{1.0}Fe_2O_4$	0	8.39503	1.64	1.95	1.1

spinel lattice. The ionic radius of Mn^{2+}, Zn^{2+} and Fe^{3+} are, respectively, 0.81, 0.74 and 0.68 Å, which are well above the void size of tetrahedral A-site (0.28 Å) and octahedral B-site (0.52 Å). Thus, introduction of Mn^{2+}, Zn^{2+} and Fe^{3+} into the defects sites results into the strained lattice. Owing to the smaller ionic radius of Zn ion, amongst the bivalent metal ions (Zn^{2+}, Mn^{2+}), Zn occupies the tetrahedral A-sites, while Mn^{2+} which are supposed to occupy the tetrahedral sites only, now also partially occupies the octahedral sites. The fraction of octahedral sites occupied by the Mn^{2+} ions or the amount of tetrahedral sites occupied by the Fe^{3+} ions, referred as degree of inversion 'δ' is responsible for this observed change in lattice parameters. Rath *et al.* [19] have previously reported decrease in lattice parameter with increasing Zn ion substitution, which they have attributed to the replacement of Mn^{2+} cations having a larger ionic radii ($r = 0.082$ nm) by Zn^{2+} cations having smaller ionic radii ($r = 0.074$ nm). However, they have not evaluated distributions of occupancies of bivalent and trivalent metal ions between tetrahedral A-sites and octahedral B-sites to support their conclusion. The opposite trend in lattice parameter variation observed in this Letter could be because of the compensation of lattice strain decrease due to Zn substitution at Mn sites by the corresponding increase in it due to different degree of inversion with increasing Zn substitution in spinel matrix of MZ NPs. Degree of inversion 'δ' is also responsible for variation in the magnetic characteristics of MZ NPs explained in the latter section of this Letter.

To further probe the effect of Zn substitution on the particle size and hence on their magnetic characteristics, analysis of peak broadening in each diffractogram was performed by adopting the Williamson–Hall (W–H) approach [26]. According to the W–H approach, crystallite size and lattice strain both contributes to the X-ray peak broadening ($\beta_{1/2}$). X-ray line broadening is the sum of contribution from crystallite size and lattice strain present in the sample, i.e.

$$\beta_{1/2} = \beta\text{size} + \beta\text{strain} \tag{3}$$

where $\beta\text{size} = \lambda/(L\cos\theta)$ and $\beta\text{strain} = 4\eta\tan\theta$

$$\beta_{1/2}\cos\theta = 4\eta\sin\theta + \lambda/L \tag{4}$$

where λ is the wavelength of X-rays, L is the full-width half maximum of each diffraction peaks, θ is the angle of diffraction, η represents the lattice strain and $\beta_{1/2}$ is the average crystallite size of NPs. If $\beta_{1/2}\cos\theta$ is plotted against $\sin\theta$, the slope of the line and intercept will provide estimation of the lattice strain and crystallite size of the NPs, respectively. The variation in crystallite size of MZ NPs obtained from W–H plot as a function of x is also shown in Fig. 2. The highest crystallite size (19 nm) is observed for $x = 1$ in MZ NPs, which is within the superparamagnetic limit of 25 nm generally observed in MZ NPs [26, 27]. The crystallite size of MZ NPs decreases with increasing Zn-content in the spinel matrix of MZ. The crystallite size varies between 9 and 19 nm for different degrees of Zn substitution in MZ NPs. This variation in crystallite

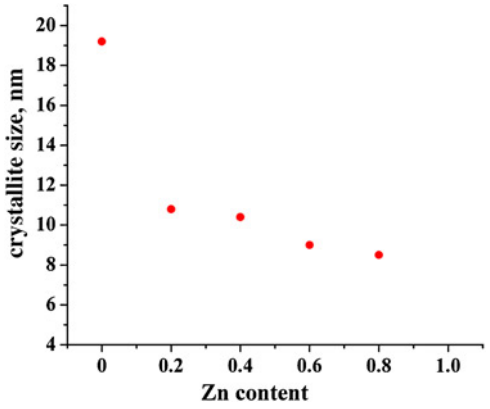

Fig. 2 *Effect of Zn substitution on crystallite size of $Mn_{1-x}Zn_xFe_2O_4$ ($x = 0$–1) NPs*

size indicates that Zn also acts as grain growth inhibitor during the synthesis of MZ NPs [28]. These results are also in well agreement with those reported in literature [20]. From XRD studies following conclusions have been drawn. Diffractograms were further refined by Rietveld refinement method by using Fullprof suite programme [29, 30]. With increasing in the degree of Zn substitution, the lattice parameter increases due to increase in the lattice strain caused degree of inversion due to the partial occupation of both the octahedral and tetrahedral sites by larger ionic radii Mn^{2+} ions. Increasing Zn substitution in the spinel lattice also causes decrease in the crystallite size of MZ NPs which will be later correlated with their magnetic properties.

Morphology of the NPs is another critical parameter that has significant influence of magnetic characteristics and at nanoscale this becomes even more influential due to morphological dependence of quantum size effects. TEM is performed to understand the morphology of as-synthesised MZ NPs. Fig. 3 shows the TEM image and (SAED) pattern of as-synthesised MZ NPs. The TEM micrograph of $Mn_{0.6}Zn_{0.4}Fe_2O_4$ NPs is shown in Fig. 3 as a representative case. TEM images of other MZ NPs are identical to that shown in Fig. 3 and hence omitted from the Letter. As can be seen in the TEM micrograph as-prepared sample has near spherical morphology. Heavy clustering of NPs is also observed in the micrograph, which is caused by the dipole–dipole interaction of small magnetic NPs. This is a typical characteristic of bare magnetic NPs in a colloidal state.

Magnetic properties (saturation magnetisation, Curie temperature, coercivity and retentivity) of MZ NPs depend on several factors. The most influential one are the degree of Zn substitution

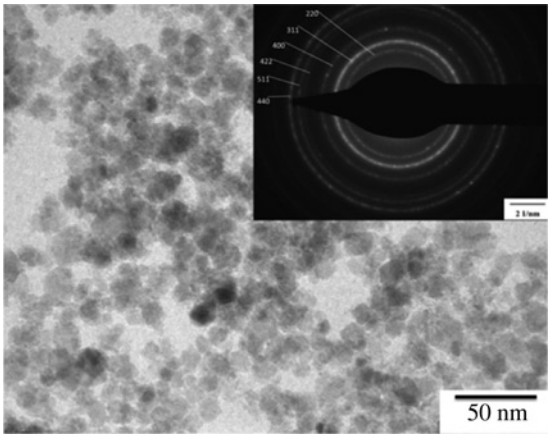

Fig. 3 *TEM image and electron diffraction pattern (inset) of $Mn_{0.6}Zn_{0.4}Fe_2O_4$ NPs*

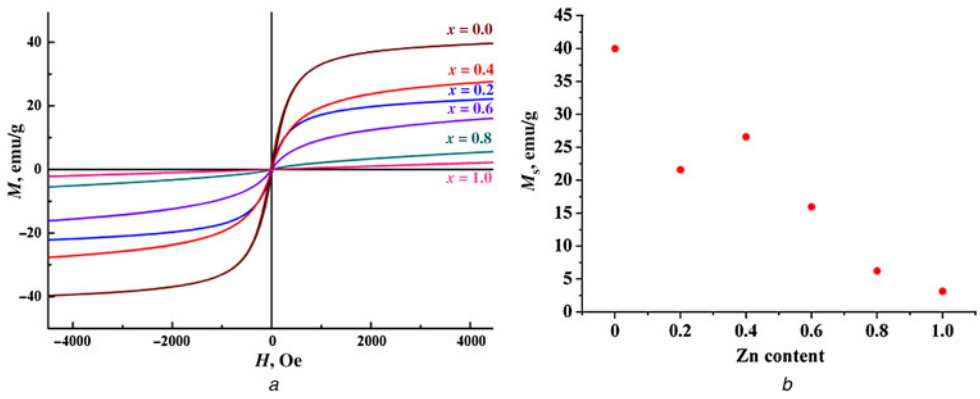

Fig. 4 *Specific magnetisation curves of the as-synthesized MZ NPs*
a Magnetisation curves of $Mn_{1-x}Zn_xFe_2O_4$ ($x = 0$–1) NPs
b Saturation magnetisation as a function of Zn- content

and degree of inversion 'δ' in addition to crystallite size and morphology of NPs. We have previously understood the effect of Zn substation on crystallite size and degree of inversion 'δ' on the lattice parameter. Now, we will correlate them with the magnetic characteristics of MZ NPs. Morphology of NPs is independent of the Zn substation and hence will not be considered any further. The specific magnetisation curves of the as-synthesised MZ NPs obtained from room temperature VSM measurements are shown in Fig. 4*a*. No hysteresis is observable in any of the samples irrespective of the degree of Zn substitution, indicating the superparamagnetic behaviour of all the as-synthesised MZ NPs [4, 5]. In each *M*–*H* curve, with increasing applied field, the magnetisation of the NPs increases exponentially. Magnetisation of the NPs undergo saturation around $H = 4.5$ KOe. The variation in the saturation magnetisation (M_s) of MZ NPs as a function of degree of Zn substitution is plotted in Fig. 4*b*. From this plot, it can be observed that the saturation magnetisation of MZ NPs strongly depends on the degree of Zn substitution. For small degree of Zn substitution, i.e. $x = 0.2$–0.4, the M_s of the MZ NPs increases with increase in the degree of Zn substitution. However, the saturation magnetisation of MZ NPs decreases with further increase in the degree of Zn substitution ($x > 0.4$).

Saturation magnetisation of NPs depends on their magnetic moment and exchange interaction. In normal, spinel bivalent metal ions (M^{2+}) occupy all the A-site and Fe^{3+} ions occupy the B-site. It can be schematically represented as

$$\begin{array}{c} \mathrm{A\ \ [\ \ B\ \ ]} \\ \mathrm{Me^{2+}[Fe^{3+}]O^{2-}{}_4} \\ \downarrow \quad \uparrow \ \ 0 \end{array}$$

In the inverse spinel, one half of the Fe^{3+} ions occupy A-site and another half is at B-site. Their magnetic moments are mutually compensated and the resulting moment of the NPs is because of the magnetic moments of bivalent cations Me^{2+} at the B-site

$$\begin{array}{c} \mathrm{A[\quad B\quad]} \\ \mathrm{Fe^{3+}[Me^{2+}Fe^{3+}]O^{2-}{}_4} \\ \downarrow \quad \uparrow \ \uparrow \ 0 \end{array}$$

In mixed spinel bivalent metal ions M^{2+} and Fe^{3+} ions occupy both A- and B-sites. The schematic formula for such mixed spinel is

$$\begin{array}{c} \mathrm{A\qquad [\qquad B\qquad]} \\ \mathrm{M^{2+}{}_{1-\delta}Fe^{3+}{}_{\delta}[Mn^{2+}{}_{\delta}Fe^{3+}{}_{1-\delta}Fe^{3+}]O^{2-}{}_4} \\ \downarrow \quad \downarrow \quad \uparrow \qquad \uparrow \ \uparrow \ 0 \end{array}$$

where δ is the degree of inversion. It represents fraction of Fe^{3+} present at A-site. In all these spinel structures, sub-lattice A is at tetrahedral sites and sub-lattice B is at octahedral sites. Interaction between A and B sub-lattices in spinel structures consist of inter-sub-lattice (A–B) super–exchange interactions and intra-sub-lattice (A–A) and (B–B) exchange interactions. Amongst these, the inter-sub-lattice (A–B) interaction is the strongest. (A–A) is relatively weak as compared with (A–B) interaction. It is generally ten times weaker than (A–B) interaction. (B–B) interaction is the weakest amongst the three [31, 32].

Bulk $MnFe_2O_4$ is expected to have normal spinel structure. When the size of $MnFe_2O_4$ decreases to several nanometres, it transformed into mixed spinel structure with degree of inversion, $\delta = 0.1$–0.3 [33]. From our X-ray refined data, the δ value for $MnFe_2O_4$ is 0.22 (Table 1). This means that in $MnFe_2O_4$ NPs, some of the Fe^{3+} ions which are at B-site in normal spinel will now shift to A-site

$$\begin{array}{c} \mathrm{A\quad [\qquad B\qquad]} \\ \mathrm{Mn^{2+}{}_{0.78}Fe^{3+}{}_{0.22}[Mn^{2+}{}_{0.18}Fe^{3+}{}_{0.78}Fe^{3+}]O^{2-}{}_4} \\ \downarrow \quad \downarrow \qquad \uparrow \qquad \uparrow \qquad \uparrow \quad 0 \end{array}$$

Accumulation of Fe^{3+} ions at A-site results into strong $Fe_A{}^{3+}$–$Fe_B{}^{3+}$ inter-lattice super–exchange interaction. As the (A–B) interactions are much stronger as compared with $Mn_A{}^{2+}$–$Fe_B{}^{3+}$ interactions and other (A–A) and (B–B) interactions, this would lead to highest saturation magnetisation amongst the studied MZ NPs [34]. However, the observed saturation magnetisation of 40 emu/g is much smaller than the M_s value of bulk $MnFe_2O_4$, which is 80 emu/g [35]. This decrease in saturation magnetisation could be caused by the formation of magnetic dead layer on the surface of NPs due to the decrease in their particle size [18, 36].

Partial substitution of Zn^{2+} ions at A-sites increases the diamagnetic contribution and reduces the Mn^{2+} ions at A-sites. This weakens the $Fe_A{}^{3+}$–$Fe_B{}^{3+}$ and $Mn_A{}^{2+}$–$Fe_B{}^{3+}$ inter-lattice exchange interactions, which result into decrease in the saturation magnetisation (21.5 emu/g) of $Mn_{0.8}Zn_{0.2}Fe_2O_4$ NPs (Fig. 4*b*)

$$\begin{array}{c} \mathrm{A\qquad [\qquad B\qquad]} \\ \mathrm{Zn^{2+}{}_{0.2}Mn^{2+}{}_{0.48}Fe^{3+}{}_{0.32}[Mn^{2+}{}_{0.32}Fe^{3+}{}_{0.68}Fe^{3+}]O^{2-}{}_4} \\ 0 \quad \downarrow \quad \downarrow \qquad \uparrow \qquad \uparrow \qquad \uparrow \quad 0 \end{array}$$

Further increase in Zn substitution ($x = 0.4$) again increases saturation magnetisation from 21.5 to 26.6 emu/g. This increase in M_s is caused by two competitive processes. Increasing Zn-content increases the diamagnetic contribution, which is contributing toward the decrease

doi: 10.1049/mnl.2016.0555

in the overall magnetisation. At the same time, this decrease in saturation magnetisation is compensated by corresponding increase in Mn_A^{2+}–Fe_B^{3+} inter-lattice exchange interactions

$$\begin{array}{cccccccc} & & A & & [& & B &] \\ Zn^{2+}_{0.4} & Mn^{2+}_{0.32} & Fe^{3+}_{0.28} & [Mn^{2+}_{0.28} & Fe^{3+}_{0.72} & Fe^{3+}] & O^{2-}_{4} \\ 0 & \downarrow & \downarrow & \uparrow & \uparrow & \uparrow & 0 & \end{array}$$

Increase in the Zn^{2+} ions at A-site lead to an increased Mn_A^{2+}–Fe_B^{3+} interaction. This enhanced A–B interaction dominates over the decreasing (A–A) interaction and thus lead to an enhancement in the overall magnetisation of $Mn_{0.6}Zn_{0.4}Fe_2O_4$ NPs. Similar results have been previously reported by Anantharaman *et al.* [37].

With further increase in Zn ($x > 0.4$), the M_s of MZ NPs decreases. Similar trend was observed by Anantharaman *et al.* [37]. They have attributed this change to transformation of mixed spinel structure to inverse spinel structure. However, they did not support their speculation with concrete experimental proofs. Contradictory to their claim, we have observed no such deviation from mixed spinel structure (except for $ZnFe_2O_4$, which is normal spinel) as previously concluded from X-ray analysis. We attribute this decreasing saturation magnetisation of MZ NPs with increasing Zn substitution at tetrahedral A-site to enhanced diamagnetic contribution of Zn, weakening A–B and A–A interactions.

In $ZnFe_2O_4$, i.e. $x = 1$; there is no (A–B) or (A–A) interactions. The only possible interaction is the very weak (B–B) interaction between the two Fe^{3+} ions present at B-site. As this interaction is very week, it shows a typical paramagnetic behaviour (Fig. 4*a*)

$$\begin{array}{cccccc} A & & [& B &] & \\ Zn^{2+} & [Fe^{3+} & Fe^{3+}] & O_4^{2-} & & \\ 0 & \uparrow & \uparrow & 0 & & \end{array}$$

In some cases small magnetism is reported in $ZnFe_2O_4$ NPs [38, 39]. For example, after fast quenching, a small part of Zn^{2+} may remain at the B-site and corresponding part of Fe^{3+} at the A-site. Typical degree of inversion 'δ' reported in the literature is of the order of 0.1 [40]. This type of $ZnFe_2O_4$ manifests non-compensated ferri or anti-ferromagnetism; however, in our case we did not find any evidence of such non-compensated spins.

To further probe the superparamagnetic characteristics of MZ NPs, their coercivity (H_c) and retentivity (M_r) have been determined from the *M*–*H* loops in Fig. 4*a*. Both H_c and M_r are plotted as a function of Zn-content in Fig. 5. For $x > 0$, H_c and M_r have near zero values indicating that the as-synthesised MZ NPs are superparamagnetic. For $x = 0$, i.e. $MnFe_2O_4$ NPs, both H_c and M_r have slightly higher values. The origin of this small ferrimagnetism could be ascribed to the presence of NPs having larger grains as

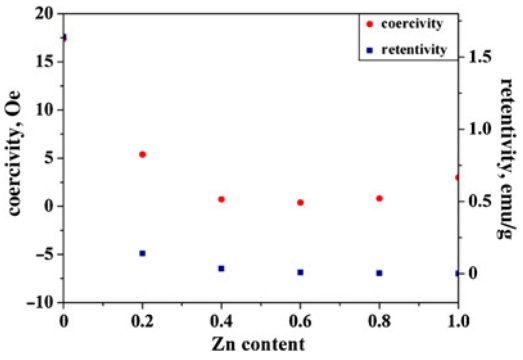

Fig. 5 *Coercivity and retentivity of $Mn_{1-x}Zn_xFe_2O_4$ (x = 0–1) NPs*

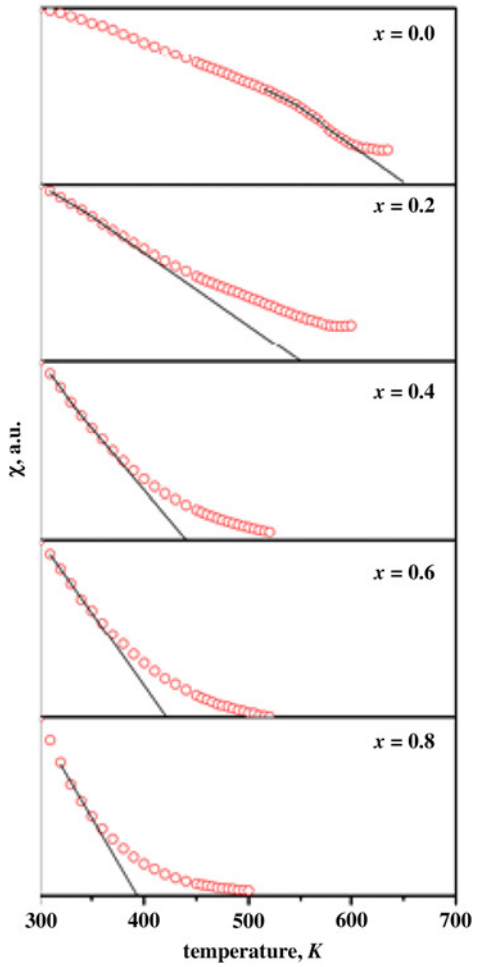

Fig. 6 *Plot of magnetic susceptibility (χ) as a function of temperature for $Mn_{1-x}Zn_xFe_2O_4$ (x = 0–0.8) NPs. Each χ against T curve is linearly extrapolated to obtain the Curie temperature of magnetic NPs*

evidenced from their relatively larger crystallite size. Another important magnetic property of MZ NPs that too depend on the degree of Zn substitution is their Curie temperature (T_c). Curie temperature of MZ NPs has also been determined from high-temperature VSM measurements. Fig. 6 shows the normalised susceptibility (χ) of various MZ NPs as a function of temperature. The linear region of $\chi \rightarrow T$ curves has been extrapolated and its intercept on the *x*-axis gives the Curie temperature. Curie temperature of MZ NPs as a function of Zn-content '*x*' is also shown in Fig. 7. Curie temperature of $MnFe_2O_4$ is highest (652 K), which monotonously

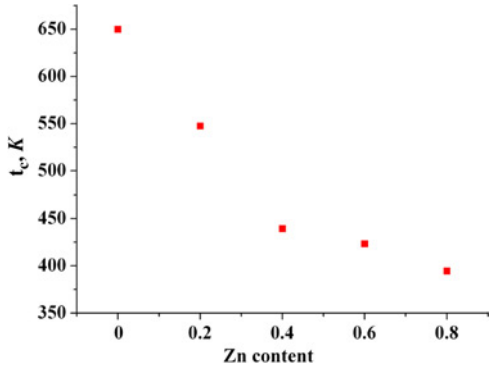

Fig. 7 *Effect of Zn-content on the Curie temperature of $Mn_{1-x}Zn_xFe_2O_4$ (x = 0–0.8) NPs*

decreases with the increase in the Zn-content. The T_c of MZ NPs drops to 361 K for $x = 0.8$. MZ NPs with Zn-content have stronger (A–B) exchange interaction, which is also responsible for their high Curie temperature. As the Zn-content in the MZ NPs increases, the (A–B) intra-lattice exchange interaction weakens leading to decrease in their Curie temperature.

5. Conclusion: Irrespective of degree of Zn substitution, MZ NPs crystallises into mixed spinel structure with degree of inversion 'δ' 0.15–0.32. Saturation magnetisation and Curie temperature of MZ NPs are strongly correlated with the degree of inversion and exchange interactions between the magnetic ions, while the coercivity and remanence are independent of it and only depends on crystallite size. Both saturation magnetisation and Curie temperature decreases with increasing Zn substitution into spinel matrix. It is attributed to the weakening of strong (A–B) inter-lattice super–exchange interaction instead partial substitution of Zn at octahedral Mn sites.

6. Acknowledgments: Authors are thankful to the Council of Scientific and Industrial Research, New Delhi [scheme no. 03 (1226)/12/ERM-II] and the Department of Science and Technology (DST FIST scheme no. SR/FST/PSI-176/2012) for the financial support.

7 References

[1] Deraz N.M.: 'Effects of magnesia addition on structural, morphological and magnetic properties of nano-crystalline nickel ferrite system', *Ceram. Int.*, 2012, **38**, p. 511
[2] Kooti M., Afshari M.: 'Phosphotungstic acid supported on magnetic nanoparticles as an efficient reusable catalyst for epoxidation of alkenes', *Mater. Res. Bull.*, 2012, **47**, p. 3473
[3] Rath C., Sahu K.K., Anand S., *ET AL.*: 'Preparation and characterization of nanosize Mn–Zn ferrite', *J. Magn. Magn. Mater.*, 1999, **202**, p. 77
[4] Jeyadevan B., Chinnasamy C.N., Shinoda K., *ET AL.*: 'Mn–Zn ferrite with higher magnetization for temperature sensitive magnetic fluid', *J. Appl. Phys.*, 2003, **93**, p. 8450
[5] Upadhyay T., Upadhyay R.V., Mehta R.V., *ET AL.*: 'Characterization of a temperature-sensitive magnetic fluid', *Phys. Rev. B*, 1997, **55**, p. 5585
[6] Rozman M., Drofenik M.: 'Hydrothermal synthesis of manganese zinc ferrites', *J. Am. Ceram. Soc.*, 1995, **78**, p. 2449
[7] Thakur A., Singh M.: 'Preparation and characterization of nanosize $Mn_{0.4}Zn_{0.6}Fe_2O_4$ ferrite by citrate precursor method', *Ceram. Int.*, 2003, **29**, p. 505
[8] Makovec D., Kosak A., Drofenik M.: 'The preparation of MnZn-ferrite nanoparticles in water–CTAB–hexanol microemulsions', *Nanotechnology*, 2004, **15**, p. 160
[9] Auzans E., Zins D., Massart R.: 'Synthesis and properties of Mn–Zn ferrite ferrofluids', *J. Mater. Sci.*, 1999, **34**, p. 1253
[10] Mangalaraja R.V., Ananthakmar S., Manohar P., *ET AL.*: 'Characterization of $Mn_{0.8}Zn_{0.2}Fe_2O_4$ synthesized by flash combustion technique', *Mater. Sci. Eng. A*, 2004, **367**, p. 301
[11] Lin W.H., Jean S.K.J., Hwang C.S.: 'Phase formation and composition of Mn–Zn ferrite powders prepared by hydrothermal method', *J. Mater. Res.*, 1999, **14**, p. 204
[12] Deraz N.M., Alarifi A.: 'Microstructure and magnetic studies of zinc ferrite nano-particles', *Int. J. Electrochem. Sci.*, 2012, **7**, p. 6501
[13] Shokrollahi H.: 'Structure, synthetic methods, magnetic properties and biomedical applications of ferrofluids', *Mater. Sci. Eng. C*, 2013, **33**, p. 2476
[14] Deraz N.M., Alarifi A.: 'Synthesis and characterization of pure and Li_2O doped $ZnFe_2O_4$ nanoparticles via glycine assisted route', *Polyhedron*, 2009, **28**, p. 4122
[15] Iyer R., Desai R., Upadhyay R.V.: 'Low temperature synthesis of nanosized $Mn_{1-x}Zn_xFe_2O_4$ ferrites and their characterizations', *Bull. Mater. Sci.*, 2009, **32**, p. 141
[16] Mathew D.S., Juang R.S.: 'An overview of the structure and magnetism of spinel ferrite nanoparticles and their synthesis in microemulsions', *Chem. Eng. J.*, 2007, **129**, p. 51
[17] Attia S.M.: 'Study of cation distribution of Mn–Zn ferrites', *Egypt. J. Solids*, 2006, **29**, p. 329
[18] Xuan Y., Li Q., Yang G.: 'Synthesis and magnetic properties of Mn–Zn ferrite nanoparticles', *J. Magn. Magn. Mater.*, 2007, **312**, p. 464
[19] Rath C., Anand S., Das R.P., *ET AL.*: 'Dependence on cation distribution of particle size, lattice parameter, and magnetic properties in nanosize Mn–Zn ferrite', *J. Appl. Phys.*, 2002, **91**, p. 2211
[20] Gopalan E.V., Al-Omari I.A., Malini K.A., *ET AL.*: 'Impact of zinc substitution on the structural and magnetic properties of chemically derived nanosized manganese zinc mixed ferrites', *J. Magn. Magn. Mater.*, 2009, **321**, p. 1092
[21] Varshney D., Verma K., Kumar A.: 'Structural and vibrational properties of $Zn_xMn_{1-x}Fe_2O_4$ ($x = 0.0$, 0.25, 0.50, 0.75, 1.0) mixed ferrites', *Mater. Chem. Phys.*, 2011, **131**, p. 413
[22] Mazz K., Mumtaz A., Hasanin S.K., *ET AL.*: 'Synthesis and magnetic properties of cobalt ferrite ($CoFe_2O_4$) nanoparticles prepared by wet chemical route', *J. Magn. Magn. Mater.*, 2007, **308**, p. 289
[23] Kim Y.I., Kim D., Lee C.S.: 'Synthesis and characterization of $CoFe_2O_4$ magnetic nanoparticles prepared by temperature-controlled coprecipitation method', *Physica B*, 2003, **337**, p. 42
[24] Arulmurugan R., Vaidyanathan G., Sendhilnathan S., *ET AL.*: 'Mn–Zn ferrite nanoparticles for ferrofluid preparation: study on thermal–magnetic properties', *J. Magn. Magn. Mater.*, 2006, **298**, p. 83
[25] Chand M., Kumar A., Annveer, Kumer S., *ET AL.*: 'Investigations on $Mn_xZn_{1-x}Fe_2O_4$ ($x = 0.1$, 0.3 and 0.5) nanoparticles synthesized by sol–gel and co-precipitation methods', *Indian J. Eng. Mater. Sci.*, 2011, **18**, p. 385
[26] Smit J., Wijn H.P.J.: 'Ferrites-physical properties of ferromagnetic oxides in relation to their technical applications' (Wiley, New York, 1959)
[27] Suryanarayana C., Norton M.G.: 'X-ray diffraction a practical approach' (Plenum Press, New York and London, 1998), p. 213
[28] Daniil M., Zhang Y., Okumura H., *ET AL.*: 'Effect of grain growth inhibitors on the hysteresis properties of $Nd_{10}Fe_{82}C_6B_2$ melt-spun alloys', *IEEE Trans. Magn.*, 2002, **38**, p. 2973
[29] Gomes J.A., Sousa M.H., Tourinho F.A., *ET AL.*: 'Rietveld structure refinement of the cation distribution in ferrite fine particles studied by X-ray powder diffraction', *J. Magn. Magn. Mater.*, 2005, **289**, p. 184
[30] Kim J., Seo J., Cheon J., *ET AL.*: 'Rietveld analysis of nano-crystalline $MnFe_2O_4$ with electron powder diffraction', *Bull. Korean Chem. Soc.*, 2009, **30**, p. 183
[31] Atif M., Hasanian S.K., Nadeem M.: 'Magnetization of sol–gel prepared zinc ferrite nanoparticles: effects of inversion and particle size', *Solid State Commun..*, 2006, **138**, p. 416
[32] Ammar S., Jouini N., Fievet F., *ET AL.*: 'Magnetic properties of zinc ferrite nanoparticles synthesized by hydrolysis in a polyol medium', *J. Phys., Condens. Matter*, 2006, **18**, p. 9055
[33] Daliya S.M., Juang R.S.: 'An overview of the structure and magnetism of spinel ferrite nanoparticles and their synthesis in microemulsions', *Chem. Eng. J.*, 2007, **129**, p. 51
[34] Jianjun L., Hongming Y., Guodong L., *ET AL.*: 'Cation distribution dependence of magnetic properties of sol–gel prepared $MnFe_2O_4$ spinel ferrite nanoparticles', *J. Magn. Magn. Mater.*, 2010, **322**, p. 3396
[35] Brabers V.A.M.: 'Handbook of magnetic materials' (Elsevier Science, Amsterdam, 1995), vol. **8**
[36] Nogues J., Sort J., Langlias V., *ET AL.*: 'Exchange bias in nanostructures', *Phys. Rep.*, 2005, **422**, p. 65
[37] Guillaud C., Creveaux H.: 'Proprietes ferromagnetiques des ferrites mixtes de Co et de Zn et de Mn et Zn', *C. R. Acad. Sci. (Paris)*, 1950, **230**, p. 1458
[38] Anantharaman M.R., Jagadeeshan S., Malini K.A., *ET AL.*: 'On the magnetic properties of ultra-fine zinc ferrites', *J. Magn. Magn. Mater.*, 1998, **189**, p. 83
[39] Lotgering F.K.: 'The influence of Fe^{3+} ions at tetrahedral sites on the magnetic properties of $ZnFe_2O_4$', *J. Phys. Chem. Solids*, 1966, **27**, p. 139
[40] Rabkin L., Soskin S., Epsstein B.: 'Ferrites: structure, properties and technology Leningrad', 1968, p. 263 (in Russ.)

doi: 10.1049/mnl.2016.0555